# NUMERICAL SIMULATION OF A FALLING SPHERE IN AIR

**Takashi Nomura[1] and Takuma Motohashi[2]**

[1] Department of Civil Engineering, College of Science and Technology
Nihon University, Tokyo 101-8308, Japan
nomura@civil.cst.nihon-u.ac.jp
[2] Okumura Corporation, Osaka, 545-8555, Japan

**Key Words:** *Fluid-structure interaction, FEM, Falling sphere, Terminal velocity.*

In order to predict the flying behavior of debris through wind by numerical simulation, a fluid-structure interaction method is developed. The main idea behind the present method is that the domain of the flow simulation is deployed over a limited area around the flying body which is wide enough to evaluate the aerodynamic forces, and the computational domain moves with the flying body. The numerical flow simulation method employed in the present study is the finite element method based on the variational multi-scale method [1]. The ALE method is applied to handle the moving mesh. The coupling procedure is a kind of partially coupled staggered scheme [2]. In order to examine the fundamental feature of the present method, the present numerical method is applied to the problem of free fall of a sphere in the still air as well as in a uniform lateral flow.

In the problem of a falling sphere in the still air, it is expected that, when the upward drag force and the gravitational force are balanced, the falling velocity $\dot{z}$ of the sphere will reach the terminal velocity $\dot{z}_T = \sqrt{\frac{4\beta}{3C_D}}\sqrt{gD}$ where $C_D$ is the drag coefficient of the sphere and $\beta = \rho_b/\rho_a$ is the ratio of the sphere density $\rho_b$ to the air density $\rho_a$. The ratio $\beta$ is two in the following computation.

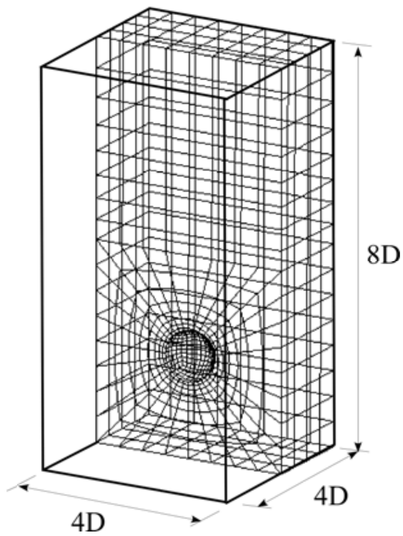


Fig. 1 Finite element mesh.

Figure 1 shows the finite element mesh which consists of 4122 hexahedral elements. The slip condition is specified on the four vertical boundaries. The top and the bottom horizontal boundaries are the traction free boundaries, and the sphere surface is the no-slip boundary. The vertical component of all the nodal mesh velocity is set to the vertical velocity $\dot{z}$ of the sphere.

Figure 2 shows two cases of the computed history of the

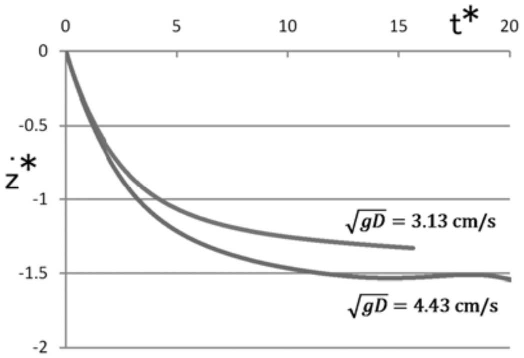


Fig.2 Computed nondimensional falling velocity of the sphere.

Table 1 Computed characteristic values

| $\sqrt{gD}$ (cm/s) | $z_T^*$ | $C_D$ | $Re$ | $C_D \times Ta^*$ |
|---|---|---|---|---|
| 3.13 | 1.36 | 1.44 | 58.2 | 0.995 |
| 4.43 | 1.53 | 1.12 | 93.1 | 0.991 |

falling velocity, where $\dot{z}^* = \dot{z}/\sqrt{gD}$ and $t^* = t/\sqrt{D/g}$ are the non-dimensional falling velocity and the non-dimensional time, respectively. In both cases, the falling velocity of the sphere reaches the terminal velocity. The characteristic values of these two cases of computation are summarized in Table 1. The computed drag coefficients $C_D$ at the terminal velocity are close to tha values in literature [3]. $Ta^* = 3\dot{z}_T^2/4\beta gD$ is a modified Tachikawa number [4] and $C_D \times Ta^*$ should be 1 theoretically when the sphere is falling at the terminal velocity.

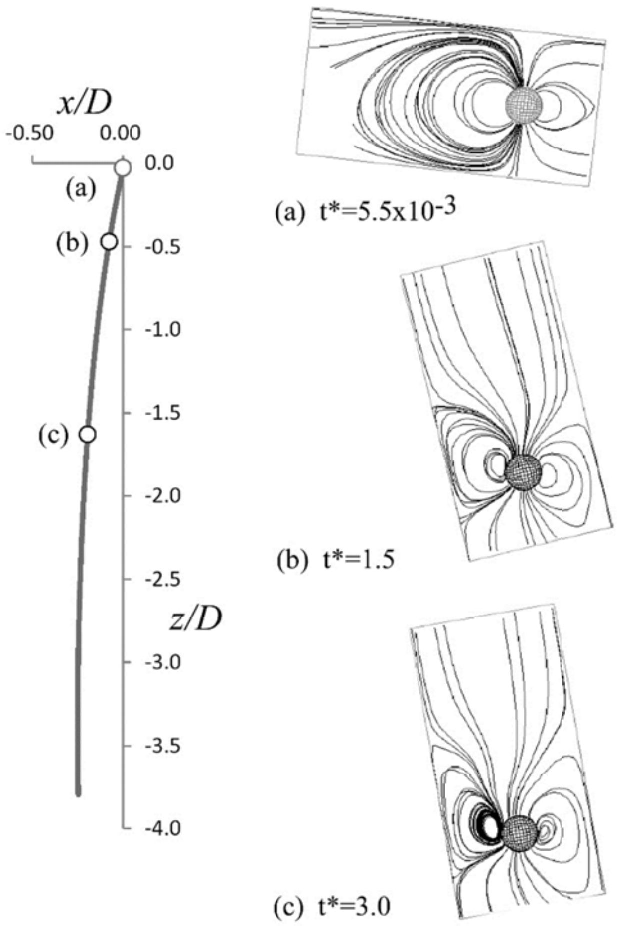


Fig.3 A falling sphere in a uniform flow: the trajectory and the computed flows at the three indicated locations.

Figure 3 shows the case of a falling sphere in a uniform lateral flow from the right to the left. In this computation, the computational domain is dynamically tilted in the direction of the relative velocity to the sphere. The computed trajectory shows a down wind motion of the sphere.

## REFERENCES

[1] Bazilevs, Y, et.al (2007) Variational multiscale residual-based turbulence modelling for large eddy simulation of incompressible flows, *Comput. Methods Appl. Mech. Engrg*, **197,** 173-201.

[2] Nomura, T (2013) Interaction of fluid and rigid body motion using ALE/VMS method, *FEF17*.

[3] Mikhailov, MD and Silva Freire, AP (2013) The drag coefficient of a sphere: An approximation using Shanks transform, *Powder Technology*, **237**, 432-435.

[4] Holmes, JD, Baker, CJ and Tamura Y (2006) Tachikawa number: A proposal, *J. Wind Engineering and Industrial Aerodynamics*, **94**, 41-47.